

# TRANSVERSE OPTICS-BASED CONTROL OF THE MICROBUNCHING INSTABILITY

A. D. Brynes\*, E. Allaria, G. De Ninno, S. Di Mitri, D. Garzella, G. Perosa, C. Spezzani  
 Elettra-Sincrotrone Trieste S.C.p.A., Trieste, Italy  
 C.-Y. Tsai

Department of Electrotechnical Theory and Advanced Electromagnetic Technology,  
 Huazhong University of Science and Technology, Wuhan, China

## Abstract

A number of recent experimental and theoretical studies have investigated novel techniques for suppressing the microbunching instability in high-brightness linac-based light sources. This instability has long been studied as one of the causes of reduced longitudinal coherence in these machines. It is commonly suppressed using a laser heater. This contribution presents recent developments which use an optics-based scheme to mitigate the microbunching instability in the FERMI free-electron laser, paving the way towards reversible beam heating techniques that could improve the performance of future machines.

## INTRODUCTION

High-brightness electron bunches are a fundamental requirement for producing high-intensity, narrow-bandwidth free electron laser (FEL) pulses [1]. The 6D beam brightness is described by the phase space volume occupied by the beam: in the transverse plane, a bright beam has a small emittance, whereas the requirements for the longitudinal properties of the beam are a high current density and a low slice energy spread [2, 3]. One of the key factors that can reduce the brightness of the electron beam as it is accelerated on its path towards the FEL undulators is the microbunching instability [1, 4, 5], which arises due to a variety of collective interactions between particles in the beam and its environment [6]. This instability can result in a beam that has a non-uniform longitudinal density profile, and an increased slice energy spread [7, 8], thereby reducing the quality of the light produced in the FEL [9, 10].

Various methods have been proposed and tested to mitigate the development of this instability, and to preserve the beam brightness up to the entrance of the FEL [11]. The most widely used of these methods is the laser heater [12, 13], a device which increases the uncorrelated slice energy spread in the beam (to an acceptable level). However, other methods can lead to the suppression of small-scale modulations in the beam without resorting to this irreversible dilution of the beam phase space [14–23]. In this contribution, a method of controlling the microbunching content in the beam is exploited at the FERMI FEL [24]. The transverse optics functions of the beam are varied along the linac-to-FEL transfer line (also known as the ‘spreader’), and it is observed that the FEL performance can be improved simply using quadrupole magnets.

\* alexander.brynes@elettra.eu

## THEORY

The one-dimensional bunching factor  $b(k)$  [25–27] is used to characterize the depth of modulations in the electron bunch as a function of wavenumber. This parameter is given by the Fourier transform of the current profile. The ratio between the final and initial bunching factors –  $b_f(k)$  and  $b_i(k)$ , respectively – is known as the microbunching gain  $G(k) = b_f(k)/b_i(k)$ . In the absence of collective effects, the final bunching factor is given by:

$$b_f(k) = b_i(k_0) \exp\left(-\frac{1}{2}(k_f R_{56} \sigma_{\delta,0})^2\right) \times \exp\left(-\frac{1}{2}k_f^2 \left[ \epsilon_{x,0} \beta_{x,0} \left( R_{51} - \frac{\alpha_{x,0}}{\beta_{x,0}} R_{52} \right)^2 - \frac{\epsilon_{x,0}}{\beta_{x,0}} R_{52}^2 \right]\right). \quad (1)$$

The  $R_{5x}$  parameters give the linear components of the  $6 \times 6$  transfer matrix [28], and  $\epsilon$ ,  $\beta$  and  $\alpha$  are the initial horizontal emittance and Twiss parameters of the beam. The final wavenumber  $k_f$  is given by  $k_i C$ , with  $C$  the compression factor of the lattice. For full derivations of the influence of the collective effects mentioned above on the microbunching gain, the reader is referred to Refs.[12, 13, 16, 25, 27, 29–32].

Coherent synchrotron radiation (CSR) [26, 27], geometric wakefields in accelerating structures [33], and longitudinal space-charge (LSC) [13, 34–36] are all examples of collective effects that can drive the microbunching instability during the electron beam acceleration and compression process.

It can be seen from Eq. (1) that the final bunching factor can be reduced by increasing either  $\sigma_{\delta,0}$ ,  $R_{56}$ , or  $\mathcal{H}_x$ . The third of these terms, otherwise known as the dispersion invariant, is given by the term in square brackets within the second exponential of Eq. (1). Previous work undertaken at FERMI [18] has demonstrated that a non-isochronous spreader line ( $|R_{56}| > 0$ ) can reduce the spectral bandwidth of the FEL pulse; in this contribution, a similar effect is observed by varying the dispersion invariant  $\mathcal{H}_x$ .

## MEASUREMENT METHODS

While a full measurement of the electron bunch longitudinal phase space, and the modulations therein, can be captured through the use of a vertical RF deflector and a bending magnet [37], this analysis method can be complicated [7, 8]. Alternatively, as mentioned above, the microbunching

Content from this work may be used under the terms of the CC-BY-4.0 licence (© 2023). Any distribution of this work must maintain attribution to the author(s), title of the work, publisher, and DOI

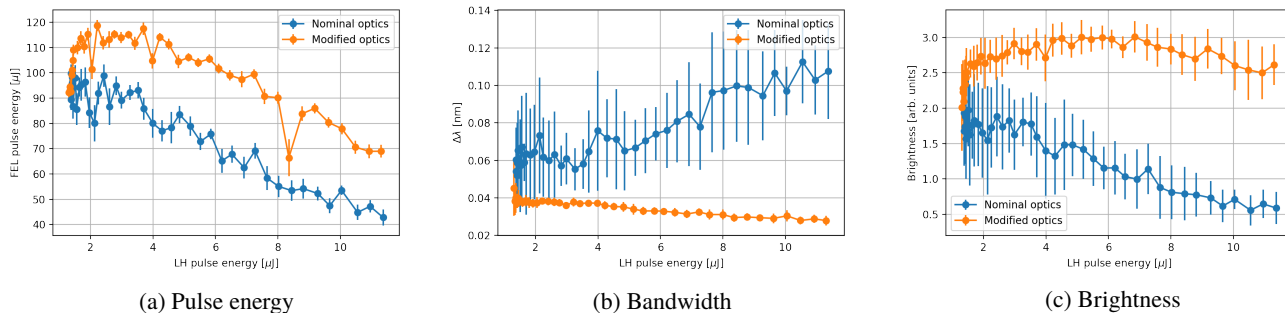


Figure 1: Performance of FEL1 as a function of laser heater pulse energy for two different transverse optics configurations in the spreader.

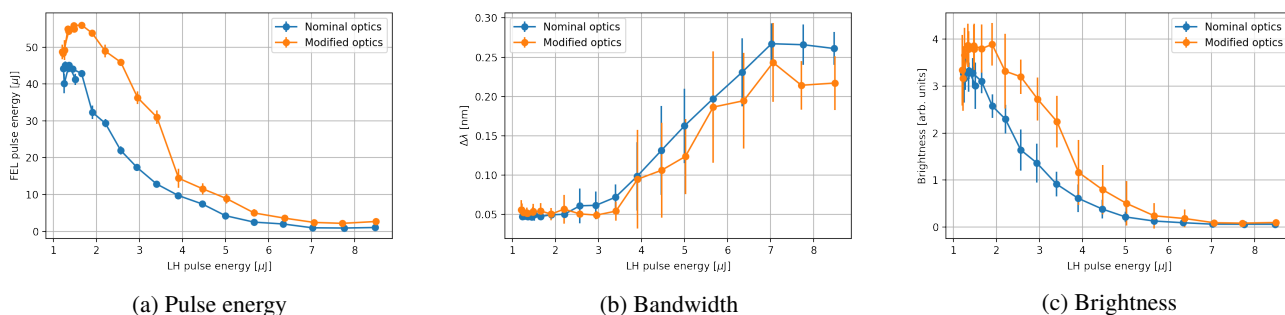


Figure 2: Performance of FEL2 as a function of laser heater pulse energy for two different transverse optics configurations in the spreader.

instability can degrade the quality of the FEL, both in terms of the pulse intensity and the bandwidth. Therefore, through the use of a laser heater, it is possible to increase the slice energy spread of the electron bunch, and thereby determine if microbunching is present in the beam [9].

A new diagnostic to measure the microbunching content in the beam, based on the generation of coherent transition radiation (CTR) and known as the Spectrometer in the InfraRed (SPIR), has recently been installed at FERMI [38–40]. CTR is generated when the electron beam passes through an aluminium foil located in the centre of the delay chicane in the FEL2 line, and the wavelength and intensity of the radiation is monitored by detectors after being dispersed through a spectrometer. The wavelength of the radiation that is generated depends on the wavelength of the modulations along the longitudinal axis of the beam, which is typically in the range 1–10 μm at this machine.

## MICROBUNCHING MITIGATION IN THE SPREADER

Two sets of experiments were performed in which the dispersion invariant  $\mathcal{H}_x$  was varied along the spreader (see Eq. (1)) by changing the transverse beam properties in the transfer line. This was achieved by altering the strengths of two quadrupole magnets in the section before the entrance

Table 1: Machine Setup for Experiments

Parameter	FEL1	FEL2	Unit
LINAC			
Bunch charge	500		pC
Initial peak current	70		A
Compression factor	8	10	
Final beam energy	1240	1535	MeV
Normalized emittance	1.2	1.4	μm-rad
FEL			
Seed wavelength	270.5	250.1	nm
Harmonic	12	8 × 5	
FEL wavelength	22.5	6.25	nm

to the spreader. The effect of varying  $\mathcal{H}_x$  on the FEL performance and the microbunching instability was characterized along both FEL lines. First, the transverse emittance at the entrance to the spreader was measured using a single-quadrupole scan [41]. Next, the strengths of two quadrupole magnets were adjusted and the beam was matched into the FEL [42]. Finally, the FEL performance (and the SPIR response) was measured as a function of laser heater pulse energy. The machine setups for the experiments on both FEL lines are summarized in Table 1.

Based on the emittance measurement and the lattice parameters in the spreader, the value of the dispersion invariant was calculated for the various optics settings using the OCELOT tracking code [43, 44]. The value of  $\mathcal{H}_x$  was calculated for the two different optics settings – the ‘nominal’ settings have two quadrupoles immediately after the emittance measurement station at the exit of the linac set to zero strength; the ‘modified’ settings do not. The modified optics have a larger dispersion invariant along the spreader, approximately 2 times larger in the case of FEL1, and around 40 % larger for FEL2.

By looking in detail at the performance of the FEL for both of these datasets, the impact of the transverse beam optics can be seen clearly – see Figs. 1 and 2 for measurements of the FEL pulse energy, bandwidth, and brightness as a function of laser heater pulse energy on both FEL lines. It can be seen that the modified optics functions in the spreader improved the FEL pulse energy and brightness in both cases. The fact that the microbunching instability is not fully suppressed with the laser heater switched off, observed already in Fig. 4, is confirmed here, as an increase in FEL performance can be achieved even with the modified optics settings for a non-zero laser heater pulse energy. An interesting discrepancy between the datasets for each FEL line, however, is the difference in the bandwidth curves (Figs. 1b and 2b): the former does not show the bandwidth increasing as a function of laser heater pulse energy for the modified optics, whereas in the latter plot, the two sets of beam optics resulted in similar bandwidth curves. This difference merits further study.

On FEL1, which does not have access to the SPIR, the FEL performance was used as the metric for judging the microbunching content in the beam. Figure 3 shows the average number of peaks in the FEL spectrum as a function of laser heater pulse energy for both optics settings. As discussed in Refs. [10, 18], the microbunching instability can induce sidebands in the FEL spectrum, and by finding local maxima in the measured spectra, it is possible to determine how clean the spectra are. With the modified optics settings, and a larger value of  $\mathcal{H}_x$ , the FEL is clearly more monochromatic, suggesting that the microbunching content has been reduced.

The second set of measurements undertaken on FEL2 provided more detailed information on the wavelength of modulations present in the bunch, thanks to the SPIR, as shown in Fig. 4. A clear peak in the intensity of the SPIR signal can be seen at around 1  $\mu\text{m}$ , and the modification of the transverse optics in the spreader can reduce this signal by approximately 90 %. The signal was not entirely removed, suggesting that there was still some residual microbunching content in the beam, and that further increasing the dispersion invariant, if compatible with maintaining acceptable optics functions in the FEL, could increase the FEL performance further. However, there are other potential explanations for this: a difference in the transverse beam size at the SPIR could have an impact on the measured signal [40]. Moreover, any current spike in the beam could produce CTR

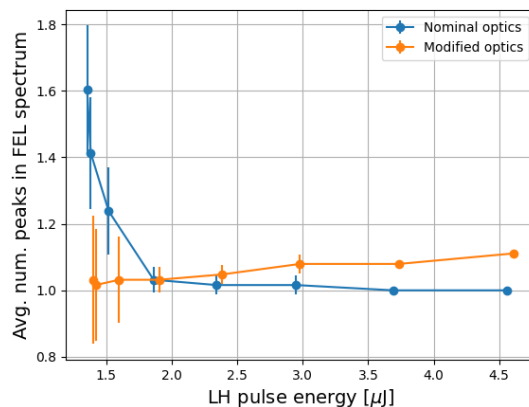


Figure 3: Average number of peaks in the spectrum of FEL1 for two different transverse optics settings in the spreader, as a function of the laser heater pulse energy. The error bars represent the standard deviation per step.

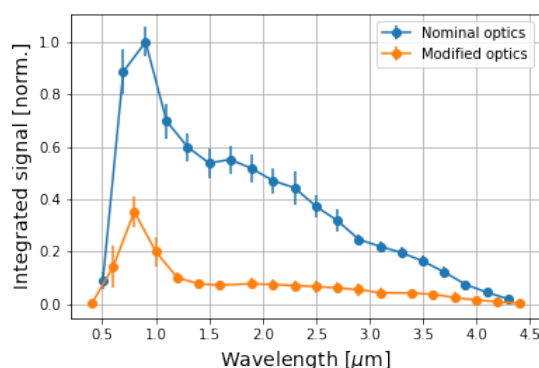


Figure 4: Integrated intensity of the SPIR as a function of IR wavelength for two different transverse optics configurations. The error bars represent the standard deviation per step.

to be observed by the IR detectors, even in the absence of any microbunching in the beam.

## CONCLUSIONS

This contribution has outlined experimental work recently undertaken at FERMI to suppress the microbunching instability through transverse control of the electron beam optics in the spreader line. It has been demonstrated that the transverse beam optics – particularly in dispersive regions – can play a key role in controlling this instability. Coupled with previous theoretical and experimental work, these results could help to pave the way towards mitigation of the microbunching instability using methods based only on beam optics. Theoretical and numerical investigations to confirm the results presented herein are currently underway.

## REFERENCES

- [1] S. D. Mitri and M. Cornacchia, *Phys. Rep.*, vol. 539, no. 1, p. 1, 2014. doi:10.1016/j.physrep.2014.01.005
- [2] P. Schmüser, M. Dohlus, J. Rossbach, and C. Behrens, *Free-electron lasers in the ultraviolet and x-ray regime*. Springer, 2014.
- [3] Z. Huang and K.-J. Kim, *Phys. Rev. Spec. Top. Accel. Beams*, vol. 10, no. 3, p. 034 801, 2007. doi:10.1103/PhysRevSTAB.10.034801
- [4] R. Akre *et al.*, *Phys. Rev. Spec. Top. Accel. Beams*, vol. 11, no. 3, p. 030 703, 2008. doi:10.1103/PhysRevSTAB.11.030703
- [5] S. D. Mitri and S. Spampinati, *Phys. Rev. Spec. Top. Accel. Beams*, vol. 17, no. 11, p. 110 702, 2014. doi:10.1103/PhysRevSTAB.17.110702
- [6] A. W. Chao, *Physics of collective beam instabilities in high energy accelerators*. Wiley, 1993.
- [7] D. Ratner *et al.*, *Phys. Rev. Spec. Top. Accel. Beams*, vol. 18, no. 3, p. 030 704, 2015. doi:10.1103/PhysRevSTAB.18.030704
- [8] A. D. Brynes *et al.*, *Sci. Rep.*, vol. 10, p. 5059, 2020. doi:10.1038/s41598-020-61764-y
- [9] Z. Huang *et al.*, *Phys. Rev. Spec. Top. Accel. Beams*, vol. 13, no. 2, p. 020 703, 2010. doi:10.1103/PhysRevSTAB.13.020703
- [10] Z. Zhang *et al.*, *Phys. Rev. Accel. Beams*, vol. 19, p. 050 701, 2016. doi:10.1103/PhysRevAccelBeams.19.050701
- [11] C.-Y. Tsai, “Suppressing CSR Microbunching in Recirculation Arcs,” in *Proc. IPAC’18, Vancouver, BC, Canada*, Vancouver, BC, Canada, Apr.-May 2018, pp. 1784–1789. doi:10.18429/JACoW-IPAC2018-WEYGBE1
- [12] E. L. Saldin, E. A. Schneidmiller, and M. V. Yurkov, *Nucl. Instrum. Meth. A*, vol. 483, no. 1, p. 516, 2002. doi:10.1016/S0168-9002(02)00372-8
- [13] Z. Huang *et al.*, *Phys. Rev. Spec. Top. Accel. Beams*, vol. 7, no. 7, p. 074 401, 2004. doi:10.1103/PhysRevSTAB.7.074401
- [14] C. Feng *et al.*, *New J. Phys.*, vol. 17, no. 7, p. 073 028, 2017. <http://iopscience.iop.org/article/10.1088/1367-2630/17/7/073028>
- [15] J. Qiang, C. E. Mitchell, and M. Venturini, *Phys. Rev. Lett.*, vol. 111, no. 5, p. 054 801, 2013. doi:10.1103/PhysRevLett.111.054801
- [16] B. Li and J. Qiang, *Phys. Rev. Accel. Beams*, vol. 23, no. 1, p. 014 403, 2020. doi:10.1103/PhysRevAccelBeams.23.014403
- [17] J. Qiang, *Nucl. Instrum. Meth. A*, vol. 1048, p. 167 968, 2023. doi:10.1016/j.nima.2022.167968
- [18] G. Perosa *et al.*, *Phys. Rev. Accel. Beams*, vol. 23, no. 11, p. 110 703, 2020. doi:10.1103/PhysRevAccelBeams.23.110703
- [19] W. Cheng *et al.*, *Nucl. Instrum. Meth. A*, vol. 1050, p. 168 145, 2023. doi:10.1016/j.nima.2023.168145
- [20] S. D. Mitri and S. Spampinati, *Phys. Rev. Lett.*, vol. 112, no. 13, p. 134 802, 2014. doi:10.1103/PhysRevLett.112.134802
- [21] S. Bettoni *et al.*, *Phys. Rev. Accel. Beams*, vol. 19, no. 3, p. 034 402, 2016. doi:10.1103/PhysRevAccelBeams.19.034402
- [22] C. Behrens, Z. Huang, and D. Xiang, *Phys. Rev. Spec. Top. Accel. Beams*, vol. 15, no. 2, p. 022 802, 2012. doi:10.1103/PhysRevSTAB.15.022802
- [23] C.-Y. Tsai *et al.*, *Phys. Rev. Accel. Beams*, vol. 20, no. 2, p. 024 401, 2017. doi:10.1103/PhysRevAccelBeams.20.024401
- [24] E. Allaria *et al.*, *J. Synch. Rad.*, vol. 22, 2015. doi:10.1107/S1600577515005366
- [25] M. Venturini, *Phys. Rev. Spec. Top. Accel. Beams*, vol. 10, no. 10, p. 104 401, 2007. doi:10.1103/PhysRevSTAB.10.104401
- [26] S. Heifets, G. Stupakov, and S. Krinsky, *Phys. Rev. Spec. Top. Accel. Beams*, vol. 5, no. 6, p. 064 401, 2002. doi:10.1103/PhysRevSTAB.5.064401
- [27] Z. Huang and K.-J. Kim, *Phys. Rev. Spec. Top. Accel. Beams*, vol. 5, no. 7, p. 074 401, 2002. doi:10.1103/PhysRevSTAB.5.074401
- [28] K. L. Brown, *SLAC-R-75*, 1982. <http://inspirehep.net/record/187522/files/slac-r-075.pdf>
- [29] M. Venturini, *Phys. Rev. Spec. Top. Accel. Beams*, vol. 11, no. 3, p. 034 401, 2008. doi:10.1103/PhysRevSTAB.11.034401
- [30] M. Venturini and J. Qiang, *Phys. Rev. Spec. Top. Accel. Beams*, vol. 18, no. 5, p. 054 401, 2015. doi:10.1103/PhysRevSTAB.18.054401
- [31] C.-Y. Tsai *et al.*, *Phys. Rev. Accel. Beams*, vol. 23, no. 12, p. 124 401, 2020. doi:10.1103/PhysRevAccelBeams.23.124401
- [32] C.-Y. Tsai *et al.*, *Phys. Rev. Accel. Beams*, vol. 20, no. 5, p. 054 401, 2017. doi:10.1103/PhysRevAccelBeams.20.054401
- [33] Z. Huang, P. Emma, M. Borland, and K.-J. Kim, “Effects of linac wakefield on CSR microbunching in the linac coherent light source,” in *Proc. PAC’03*, Portland, OR, USA, May 2003, pp. 3138–3140.
- [34] J. B. Rosenzweig *et al.*, *Nucl. Instrum. Meth. A*, vol. 393, no. 2, pp. 376–379, 1997. doi:10.1016/S0168-9002(97)00516-0
- [35] E. Saldin, E. Schneidmiller, and M. Yurkov, *Nucl. Instrum. Meth. A*, vol. 490, no. 1, p. 1, 2002. doi:10.1016/S0168-9002(02)00905-1
- [36] E. L. Saldin, E. A. Schneidmiller, and M. V. Yurkov, *Nucl. Instrum. Meth. A*, vol. 528, no. 1, p. 355, 2004. doi:10.1016/j.nima.2004.04.067
- [37] P. Craievich *et al.*, *IEEE Trans. Nucl. Sci.*, vol. 62, no. 1, p. 210, 2015. <https://ieeexplore.ieee.org/stamp/stamp.jsp?arnumber=7024948>
- [38] M. Veronese *et al.*, “Infrared spectrometer for microbunching characterization,” presented at FEL’22, Trieste, Italy, Aug. 2022, paper WEP24, unpublished.
- [39] A. D. Brynes, “Characterisation of microbunching instability at the FERMI Free Electron Laser,” presented at IPAC’23, Venice, Italy, May 2023, paper MOOG2, to appear in the proceedings.

- [40] G. Perosa *et al.*, *in preparation*, Italy, Sep. 2022, pp. 362–365.  
doi:10.18429/jacow-fe12022-wep04
- [41] M. G. Minty and F. Zimmermann, in *Measurement and Control of Charged Particle Beams*. 2003.  
doi:10.1007/978-3-662-08581-3\_4
- [42] A. D. Brynes *et al.*, “Upgrade to the transverse optics matching strategy for the FERMI FEL,” in *Proc. FEL’22*, Trieste, [43] *OCELOT*, 2018-07-30. <https://github.com/ocelot-collab/ocelot/>
- [44] I. Agapov *et al.*, *Nucl. Instrum. Meth. A*, vol. 768, p. 5, 2014.  
doi:10.1016/j.nima.2014.09.057